

Geometric Burn Control For Tokamaks

J. F. Parisi^{1,*}, J. W. Berkery¹, A. Sladkomedova², S. Guizzo³, M. R. Hardman², J. R. Ball⁴, A. O. Nelson³, S. M. Kaye¹, M. Anastopoulos-Tzani², S. A. M. McNamara², J. Dominski¹, S. Janhunen², M. Romanelli², D. Dickinson⁵, A. Diallo¹, A. Dnestrovskii², W. Guttenfelder^{6,1}, C. Hansen³, O. Myatra⁷, and H. R. Wilson⁸

¹Princeton Plasma Physics Laboratory, Princeton University, Princeton, NJ, USA

²Tokamak Energy Ltd., 173 Brook Drive, Milton Park, Oxfordshire, UK

³Department of Applied Physics & Applied Mathematics, Columbia University, New York, NY, USA

⁴Ecole Polytechnique Federale de Lausanne, Swiss Plasma Center, Lausanne, Switzerland

⁵York Plasma Institute, Department of Physics, University of York, Heslington, York, UK

⁶Type One Energy, 8383 Greenway Boulevard, Middleton, WI, USA

⁷United Kingdom Atomic Energy Authority, Culham Science Centre, Abingdon, UK and

⁸Oak Ridge National Laboratory, Oak Ridge, TN, USA

A new burn control scheme for tokamaks is described where the total fusion power is controlled by adjusting the plasma volume fraction that is packed into power dense regions. In an example spherical tokamak burning plasma, by modifying the plasma edge squareness the total fusion power is doubled at almost constant total plasma volume and fusion power density. Therefore, increased plasma squareness could be extremely beneficial to a fusion reactor and squareness control could be desirable for power load balancing. Experiments have observed the impact of increased edge squareness on modified core plasma volume, highlighting the practical relevance of this approach.

Introduction. –As electric grids incorporate more variable power resources, the value of baseload power plants with variable output rises [1–3]. For example, modern fission plant designs, historically fixed in output, now offer variable power options [4–7]. Tokamak fusion reactors, the leading candidate for commercial fusion, can also benefit from variable power output. Tokamaks confine plasma fuel at temperatures exceeding 100 million Kelvin using a toroidal magnetic cage. Various methods exist to vary power output, such as adjusting the fuel mix [8], density profiles [9], or total plasma volume. However, due to the complexity of tokamaks, these methods pose significant physics and engineering challenges. In this Article, we demonstrate how to control fusion burn with minimal disruption by altering only the plasma edge squareness ζ_0 . Increasing ζ_0 reallocates more plasma volume to power-dense regions, enhancing the burn. Squareness burn control is operationally attractive as it allows most plasma parameters, including elongation and triangularity, to remain fixed while ζ_0 varies.

Geometric Burn Control. – A tokamak reactor must confine plasma at sufficient pressure for a high fusion power density p_f . However, high p_f alone isn't enough for substantial fusion power; it must also be maintained over a large fraction of the total plasma volume V_{tot} . The largest contributions to the total fusion power

$$P_f = \int p_f dV, \quad (1)$$

come from the burn volume

$$V_{\text{burn}} \equiv \int_{\text{burn}} dV, \quad (2)$$

the volume over which p_f exceeds a value $p_{f,c}$ required for substantial fusion power. We use $p_{f,c} = 1 \text{ MW/m}^3$, which is justified later. In this work, we control P_f by

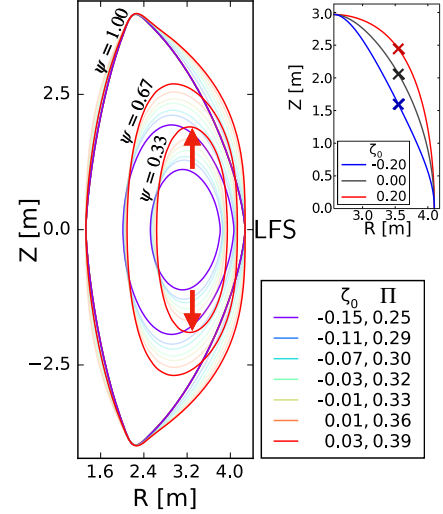


FIG. 1: Main: three flux-surfaces $\psi = [0.33, 0.67, 1.0]$ with varying edge squareness ζ_0 and Π . Red arrows show stretching of inner flux-surfaces by increasing ζ_0 . Inlet: outer flux-surfaces for three ζ_0 values.

changing the fraction of the total plasma volume V_{tot} packed into V_{burn} , given by the packing fraction

$$\Pi \equiv V_{\text{burn}}/V_{\text{tot}}. \quad (3)$$

Plasmas with $\Pi = 1$ are volume-efficient, packing the full volume into power dense regions. In contrast, $\Pi = 0$ is volume-inefficient since $V_{\text{burn}} = 0$. Thus at fixed V_{tot} ,

$$P_f \sim \Pi \langle p_f \rangle_{\text{burn}}, \quad (4)$$

where the burn average $\langle \cdot \rangle_{\text{burn}}$ is

$$\langle p_f \rangle_{\text{burn}} \equiv (1/V_{\text{burn}}) \int_{\text{burn}} p_f dV. \quad (5)$$

The key idea of this work is that controlling the plasma

edge squareness [10],

$$\zeta_0 = \arcsin(Z_m/\kappa_0 a) - \pi/4, \quad (6)$$

changes Π and thus P_f , while $\langle p_f \rangle_{\text{burn}}$ is approximately constant according to infinite-n ballooning stability [11–13], which we explain in a later section. Here, Z_m is the Z value indicated by crosses in fig. 1's inlet and $\kappa_0 = h/2a$ is the edge plasma elongation where h is the maximum plasma height and a is the minor radius.

Dedicated studies of plasma squareness are limited compared with other shape parameters, but benefits to increased ζ_0 have been identified. Squareness control is established [10, 14–17] and easier than other shape parameters because plasma x-points and maximum width and height can be fixed. Ion-scale turbulence simulations found that higher ζ_0 improves heat confinement [18], and DIII-D and MAST-U experiments show ζ_0 values typically allow higher edge pedestal pressure [19–23] and give improved core confinement [24]. Spherical tokamak design studies found positive moderate ζ_0 stabilized kink modes, allowing a 10% increase in core plasma pressure [10, 25, 26]. This benefit was discounted because of the required increase in poloidal field coil current [26, 27], but the benefits outlined in this work could change that tradeoff assessment. Furthermore, the poloidal coil currents required for the equilibria in this study are probably easier to handle since we examine significantly lower ζ_0 values. It should be noted that changes to plasma shape parameters like κ_0 or ζ_0 may require changes in other plasma parameters, such as internal inductance [28]. The work in this study is based on a representative burning spherical tokamak [29] design point, referred to as GST. The main GST parameters are on-axis toroidal field $B_{T,0} = 5$ T, plasma current $I_P = 9.8$ MA, major radius $R_0 = 3.4$ m, $a = 1.5$ m, $\kappa_0 = 2.73$, and $\delta_0 = 0.43$.

Squareness Burn Control. – Increasing squareness of the plasma edge stretches the magnetic surfaces in the plasma core. An equilibrium with $\zeta_0 = 0.03$ has core flux-surfaces that are twice as elongated as a lower ζ_0 equilibrium with $\zeta_0 = -0.15$. This is illustrated in fig. 1 – we plot surfaces of constant poloidal flux ψ with different ζ_0 and almost constant plasma volume. Comparison of the inner $\psi = 0.33$ flux surfaces for $\zeta_0 = -0.15$ and $\zeta_0 = 0.03$ shows that higher ζ_0 elongates the plasma core.

Increased core elongation more efficiently uses the core volume for fusion power by increasing V_{burn} and hence $\Pi \sim \langle \kappa \rangle_{\text{burn}}$. The total power is therefore determined mainly by p_f and κ in the burn region,

$$P_f \sim \langle \kappa \rangle_{\text{burn}} \langle p_f \rangle_{\text{burn}}, \quad (7)$$

for fixed V_{tot} . Therefore, ζ_0 , mainly through $\langle \kappa \rangle_{\text{burn}}$, determines Π and thus the fusion burn.

The physical mechanism for ζ_0 increasing Π exploits plasma properties at the low-field-side (LFS, indicated in fig. 1). With increasing plasma squareness, Π increases from 0.25 to 0.39, shown in fig. 1. The strong poloidal

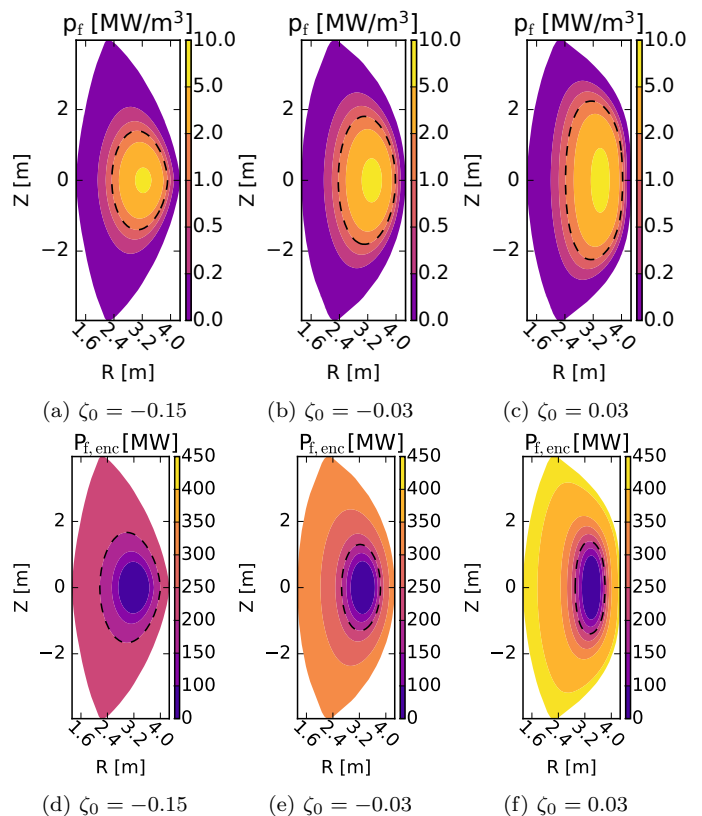


FIG. 2: Burn control scheme using plasma squareness for GST: Fusion power density (a-c) and enclosed fusion power (d-f) in increasingly square plasmas. The $p_f = 1$ MW/m³ and $P_f = 200$ MW surfaces are indicated with a dashed black contour. The total fusion power is 215 MW, 311 MW, and 403 MW for $\zeta = -0.15, -0.03$, and 0.03.

field at the LFS causes LFS flux-surfaces to be closely spaced, measured by large $|d\psi/dr|_{\text{LFS}}$ values, where r is the plasma minor radial coordinate. When ζ_0 increases, flux-surfaces are stretched vertically in order to keep $|d\psi/dr|_{\text{LFS}}$ large, indicated by red arrows in fig. 1. This effect increases for spherical tokamaks where the LFS poloidal field is particularly strong [29] and for high Shafranov shift [30], which both increase $|d\psi/dr|_{\text{LFS}}$.

The total power P_f doubles from the minimum to maximum ζ_0 values, from $P_f = 215$ MW to 403 MW. The corresponding p_f is plotted for plasmas with three ζ_0 values in fig. 2(a)-(c). The highest ζ_0 equilibrium has p_f surfaces that are much more elongated (fig. 3(b)) and it therefore has a high Π value ($\Pi = 0.39$ compared with $\Pi = 0.25, 0.32$ for $\zeta_0 = -0.15, -0.03$). Thus, higher ζ_0 equilibria efficiently distribute volume to regions of high $p_f(\psi)$, which increases P_f , despite similar $p_f(\psi)$ profiles (fig. 3(a)). For example, for $\zeta_0 = 0.03$ the flux-surface $\psi = 0.2$ has an enclosed power

$$P_{f,\text{enc}}(\psi) \equiv \int_0^{V(\psi)} p_f dV' \quad (8)$$

of 231 MW but $\zeta_0 = -0.15$ has only 98 MW (fig. 2(d)-(f) and fig. 3(c)). In fig. 3(a), vertical lines indicate the

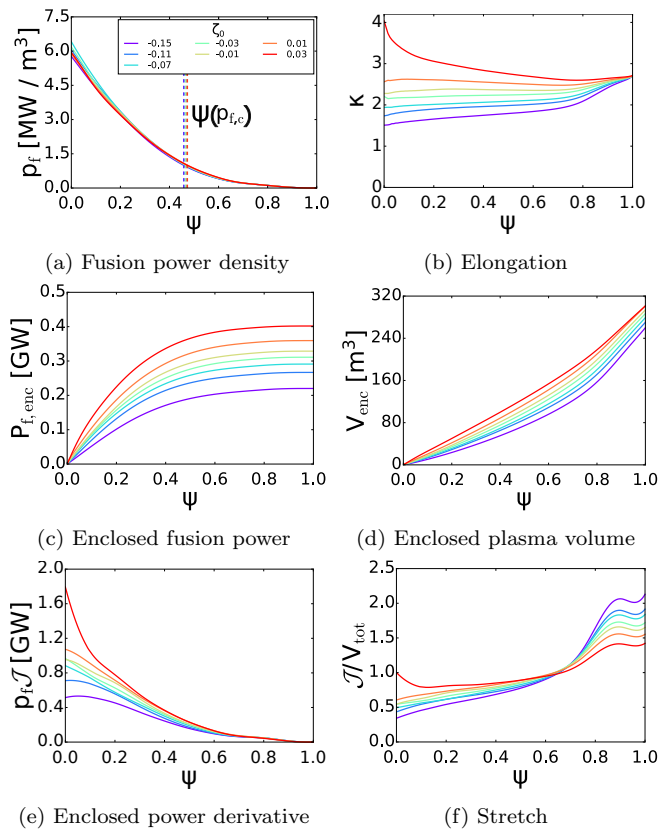


FIG. 3: GST radial profiles of power density (a), elongation (b), enclosed power (c), enclosed volume (d) and enclosed power derivative (eq. (9)) (e), and Stretch (eq. (10)).

surface ψ_{burn} where $p_{f,c} = 1$ MW/m³; for all equilibria, $P_{f,enc}(\psi_{burn})/P_f > 90\%$, indicating a good choice of $p_{f,c}$.

Higher ζ_0 equilibria enclose more fusion power by growing volume relatively quickly in the burn region but slowly outside. The Jacobian $\mathcal{J} = dV_{enc}/d\psi$ measures flux-surface growth for enclosed volume $V_{enc}(\psi) \equiv \int_0^{\psi} dV'$ (fig. 3(d)). \mathcal{J} enters the derivative of $P_{f,enc}$,

$$dP_{f,enc}/d\psi = p_f \mathcal{J}, \quad (9)$$

so larger \mathcal{J} indicates faster flux-surface volume growth, contributing more to P_f . Average contributions to P_f in the burn region are double for the highest ζ_0 than the lowest ζ_0 , shown by $p_f \mathcal{J}$ in fig. 3(e). This explains how the highest ζ_0 has double the P_f of the lowest ζ_0 . The Stretch S is the normalized rate of volume growth,

$$S = \mathcal{J}/V_{tot}, \quad (10)$$

satisfying $\int_0^1 S d\psi = 1$. Surfaces with $S > 1$ increase volume faster than the average flux-surface and those with $S < 1$ increase volume slower than average. Because $S \sim (\kappa/\kappa_0)(r/a)(B_{p,0}/B_p)$, where $B_{p,0}$ is the edge poloidal field, we expect $S \ll 1$ near the core but $S \gg 1$ at the edge. This is true for low ζ_0 equilibria, shown in fig. 3(f), but for high ζ_0 equilibria, $S \approx 1$ in V_{burn} , and increases slowly near the edge. Therefore, high ζ_0 equilibria expand plasma volume relatively quickly in the burn

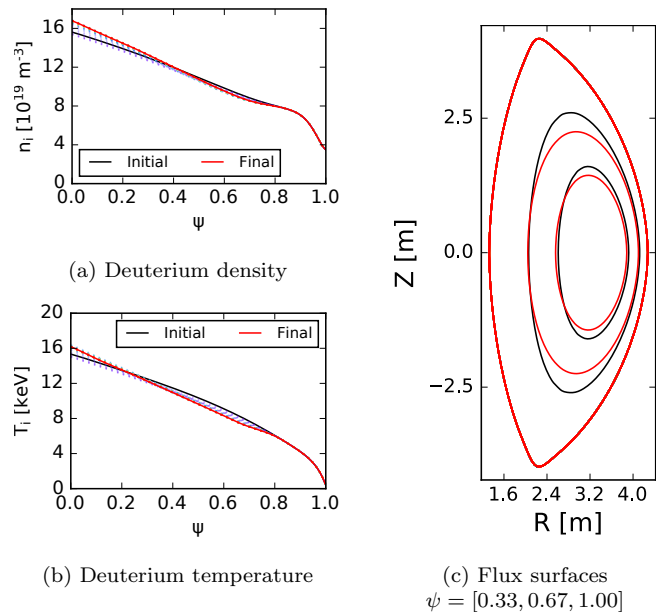


FIG. 4: Initial and final ion density and temperature for GST ((a),(b)), and equilibria (c) for $\zeta_0 = -0.01$. In (a) and (b), dotted lines are intermediate iterations. The final profile is infinite-n ballooning stable.

region, whereas low ζ_0 equilibria expand plasma volume relatively quickly in the edge where p_f is low.

Equilibrium Generation. – While this paper's focus is on new geometry insights and not integrated modeling, we ensure that the equilibria presented here clear a minimum threshold for viability: infinite-n ballooning stability [11–13]. We found that changing the equilibrium magnetic geometry by varying ζ_0 but keeping the profiles fixed caused some equilibria to be ballooning unstable. Therefore, for a fair comparison across ζ_0 values, we use an iterative scheme that generates equilibria close to the infinite-n ballooning stability boundary. For each iteration, at 10 radial locations the density and temperature gradients for thermal species are brought to the ballooning stability boundary. The fixed-boundary equilibrium is recalculated using CHEASE [31] according to the new pressure and current profiles (with consistent bootstrap current [32, 33]), subject to keeping the total plasma current I_p fixed. Increasing ζ_0 also increases the bootstrap fraction f_{bs} from $f_{bs} = 0.72$ to $f_{bs} = 0.96$ for the lowest to the highest ζ_0 . The strong increase in f_{bs} results from increased core elongation at higher ζ_0 [34]. The equilibria have five thermal species – deuterium, tritium, lithium, helium, and electrons – and a fast helium population. In fig. 4(a) and (b), we plot the deuterium temperature and density at each iteration step, and in fig. 4(c) flux-surfaces for the initial and final equilibria. To simplify analysis, we present results with fixed pressure in the pedestal edge region. Because of the effect of shape on pedestal performance [19, 35–37], we performed sensitivity analysis that showed the trends in this work still held with different pedestal heights.

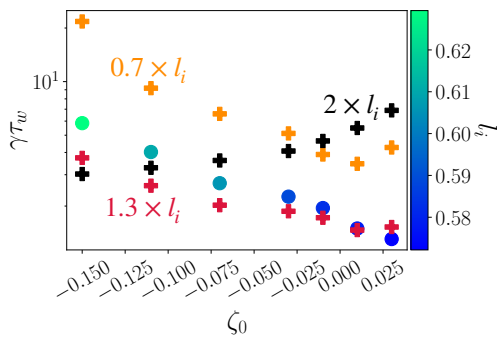


FIG. 5: Vertical stability growth rates $\gamma\tau_w$ across squareness for GST for nominal l_i (circles) and rescaled l_i (plusses).

Vertical Stability. – High plasma elongation can make a plasma more vertically unstable and trigger violent plasma termination events [38–43]. Thus, it is important to determine how ζ_0 and its strong effects on $\langle \kappa \rangle_{\text{burn}}$ (fig. 3(b)) affect vertical stability (VS). To assess VS, we use **Tokamaker** [44] to find VS growth rates for equilibria with different ζ_0 values. Free-boundary equilibria were generated and the VS growth rate $\gamma\tau_w$ calculated for the $n = 0$ mode, where the growth rate γ is normalized to the wall resistive time τ_w and n is the toroidal mode number. Shown in fig. 5, at the nominal inductance l_i values, $0.57 < l_i < 0.63$, increasing ζ_0 is stabilizing. We rescaled l_i by factors of 0.7, 1.3 and 2.0, finding that slightly higher l_i was stabilizing, but much higher and lower l_i became destabilizing. We hypothesize ζ_0 stabilization at nominal l_i values is due to a larger Shafranov shift at higher squareness, leading to stronger plasma-wall coupling. At higher l_i , the Shafranov shift is comparable for all ζ_0 values, and the effect of increased $\langle \kappa \rangle_{\text{burn}}$ with higher ζ_0 dominates. At lower l_i , the core surfaces are much more elongated for all ζ_0 values, driving vertical instability. For each ζ_0 value, the plasma wall was conformal to the plasma boundary shape. While detailed studies are required, these results suggest that the ζ_0 values investigated here are compatible with VS stabilization methods [45–48], which in current machines can control $\tau_w \lesssim 6$, although control may be somewhat degraded in future devices [49].

Experimental Equilibria. – While tokamaks have not yet produced burning plasmas, core volume packing using squareness has been observed on current devices. In fig. 6, we plot the plasma elongation, enclosed volume, and flux surfaces for two companion National Spherical Torus Experiment (NSTX) discharges [15], which differ mainly by edge squareness ($\zeta_0 = -0.01$ and $\zeta_0 = 0.10$). For the larger ζ_0 discharge, the elongation increases up to the magnetic axis (fig. 6(a)) and the enclosed plasma volume is much larger in the core (fig. 6(b)). Three flux surfaces with $\psi = [0.33, 0.67, 1.00]$ are plotted in fig. 6(c). While the fusion power is negligible in these NSTX discharges, they show that increased core volume via ζ_0 has been realized on current day experiments. Experiment-

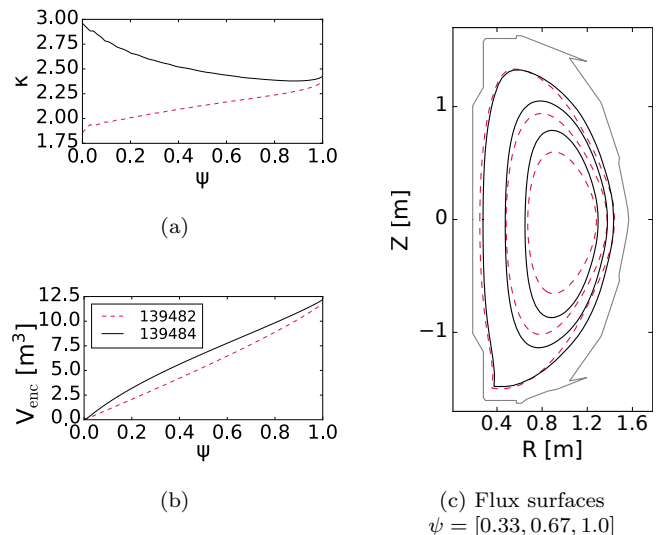


FIG. 6: Plasma elongation (a), enclosed volume (b), and flux surfaces (c) for two companion NSTX discharges (139482 @547ms, 139484 @556ms) with differing edge squareness ($\zeta = -0.01$ and $\zeta = 0.10$).

tal consideration of this effect could continue in NSTX Upgrade, which is designed to produce a wide range of squareness shapes [50].

Triangularity Scan. – Extending the concept of controlling Π and $\langle \kappa \rangle_{\text{burn}}$ with ζ_0 , we show that edge triangularity δ_0 further redistributes the volume and hence changes P_f . Starting from $\zeta_0 = -0.03$, we reconstruct equilibria with varying ζ_0 and δ_0 for fixed pressure and current profiles. Notably, in contrast to the earlier section, we have fixed $p_f(\psi)$ for these equilibria, illustrating a purely geometric effect on P_f .

Due to strong flux-expansion, negative triangularity (NT) [51, 52] gives a higher packing fraction Π . NT elongates the LFS edge flux-surface, consequently elongating core flux-surfaces. Increasing ζ_0 and reducing δ_0 expands the available core volume for fusion power, shown in fig. 7 (a). This leads to a higher $P_{f,\text{enc}}$, plotted in fig. 7(b)-(d) for three δ_0 values, each with the ζ_0 value yielding the highest P_f . The $\delta_0 = -0.5$ case yields $P_f = 520$ MW, while $\delta_0 = 0.5$ yields $P_f = 420$ MW.

From the practical perspective of a plant operator, varying δ_0 is more challenging than ζ_0 [10]. As fig. 7(a) shows, while NT increases Π at fixed p_f , varying ζ_0 for NT does not vary Π by nearly as much than at higher δ_0 values. Thus, designers of a variable power tokamak seeking a large P_f range might opt for higher δ_0 at the cost of reduced maximum P_f .

Discussion. – We have shown that geometric burn control in tokamaks is possible by manipulating the volume in power dense regions, the burn volume. Specifically, by varying the plasma squareness, a tokamak operator can change the burn volume in a manner that is not disruptive to operations. Therefore, squareness adjustability can permit power load balancing in a variable out-

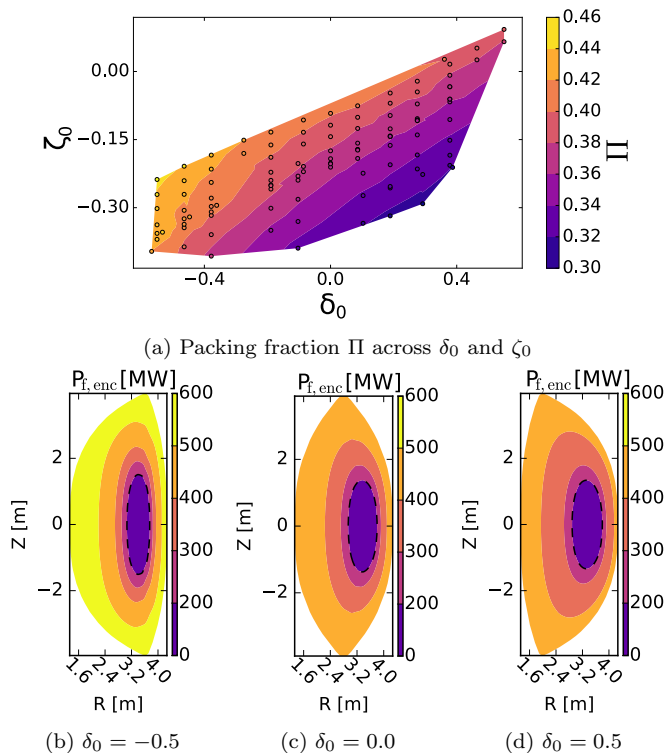


FIG. 7: (a) Packing fraction Π values for triangularity δ_0 and squareness ζ_0 scan for GST at fixed $p_f(\psi)$. (b)-(d): $P_{f,enc}$ for $\delta_0 = -0.5, 0.0, 0.5$ for ζ_0 with the highest P_f .

put reactor. We showed an example where changing the squareness doubled the total fusion power by doubling the burn volume at almost constant total volume. Additionally, a fixed power design reactor could be designed to increase or decrease fusion power through higher or lower squareness.

The concept introduced here of redistributing plasma volume is also a new way to think about tokamak ‘size.’ The two main pathways for modifying ‘size’ in modern tokamaks are the major radius R and the magnetic field strength B [53–56]. In this paper, we have introduced a complementary third way, which is the efficiency of the burn volume, which may offer an accelerated route to fusion energy in tokamaks.

Finally, while we have introduced the concept of varying the burn volume, there are many important physics and engineering areas that we have not analyzed. Fully integrated physics and engineering studies and dedicated experiments are required to determine how best to employ geometric burn control.

Acknowledgements. – This work was funded under the INFUSE program – a DOE SC FES public-private partnership – under contract no. 2706 between Princeton Plasma Physics Laboratory and Tokamak Energy Ltd. This work was supported by the U.S. Department of Energy under contract number DE-SC0022270.

Data Availability. – Data used in this analysis will be provided upon reasonable request to the first author.

* jparisi@pppl.gov

- [1] P. D. Lund, J. Lindgren, J. Mikkola, and J. Salpakari, *Renewable and Sustainable Energy Reviews* **45** (2015).
- [2] T. Levin and A. Botterud, *Energy Policy* **87** (2015).
- [3] P. J. Heptonstall and R. J. Gross, *Nature Energy* **6** (2021).
- [4] J. D. Jenkins, Z. Zhou, R. Ponciroli, R. B. Vilim, F. Ganda, F. de Sisternes, and A. Botterud, *Applied Energy* **222** (2018).
- [5] C. Cany, C. Mansilla, G. Mathonnière, and P. da Costa, *Energy* **150**, 544 (2018).
- [6] Z. Dong, B. Li, J. Li, Z. Guo, X. Huang, Y. Zhang, and Z. Zhang, *Energy* **221** (2021).
- [7] OECD, *Technical and economic aspects of load following with nuclear power plants* (OECD Publishing, 2021).
- [8] M. Maslov, E. Lerche, F. Auriemma, E. Belli, C. Bourdelle, C. Challis, A. Chomiczewska, A. D. Molin, J. Eriksson, J. Garcia, J. Hobirk, I. Ivanova-Stanik, P. Jacquet, A. Kappatou, Y. Kazakov, D. Keeling, D. King, V. Kiptily, K. Kirov, D. Kos, R. Lorenzini, E. D. L. Luna, C. Maggi, J. Mailloux, P. Mantica, M. Marin, G. Matthews, I. Monakhov, M. Nocente, G. Pucella, D. Rigamonti, F. Rimini, S. Saarelma, M. Salewski, E. Solano, Ž. Štancar, G. Stankunas, H. Sun, M. Tardocchi, D. V. Eester, and J. Contributors, *Nuclear Fusion* **63**, 112002 (2023).
- [9] H. Wilson, D. Arnold, W. Boyes, R. Chandra, H. Choudhury, N. DaSilva, C. Hansen, Y. Liu, P. Lumia, A. Nelson, *et al.*, *Bulletin of the American Physical Society* (2023).
- [10] A. D. Turnbull, Y. R. Lin-Liu, R. L. Miller, T. S. Taylor, and T. N. Todd, *Physics of Plasmas* **6**, 1113 (1999).
- [11] J. W. Connor, R. J. Hastie, and J. B. Taylor, *Proc R Soc London Ser A* **365**, 3651 (1979).
- [12] J. M. Greene and M. S. Chance, *Nuclear Fusion* **21** (1981).
- [13] R. Gaur, S. Buller, M. E. Ruth, M. Landreman, I. G. Abel, and W. Dorland, “An adjoint-based method for optimizing mhd equilibria against the infinite-n, ideal ballooning mode (<https://arxiv.org/abs/2302.07673>),” (2023), arXiv:2302.07673.
- [14] D. A. Gates, J. R. Ferron, M. Bell, T. Gibney, R. Johnson, R. J. Marsala, D. Mastrovito, J. E. Menard, D. Mueller, B. Penafior, S. A. Sabbagh, and T. Stevenson, *Nuclear Fusion* **46** (2006).
- [15] E. Kolemen, D. A. Gates, S. Gerhardt, R. Kaita, H. Kugel, D. Mueller, C. Rowley, and V. Soukhanovskii, *Nuclear Fusion* **51** (2011).
- [16] M. Ariola and A. Pironti, *Magnetic Control of Tokamak Plasmas* (Springer, 2016).
- [17] J. Degraeve, F. Felici, J. Buchli, M. Neunert, B. Tracey, F. Carpanese, T. Ewalds, R. Hafner, A. Abdolmaleki, D. de las Casas, C. Donner, L. Fritz, C. Galperti, A. Huber, J. Keeling, M. Tsimpoukelli, J. Kay, A. Merle, J. M. Moret, S. Noury, F. Pesamosca, D. Pfau, O. Sauter, C. Sommariva, S. Coda, B. Duval, A. Fasoli, P. Kohli, K. Kavukcuoglu, D. Hassabis, and M. Riedmiller, *Nature* **602** (2022).
- [18] N. Joiner and W. Dorland, *Physics of Plasmas* **17** (2010).
- [19] J. R. Ferron, M. S. Chu, G. L. Jackson, L. L. Lao, R. L. Miller, T. H. Osborne, P. B. Snyder, E. J. Strait, T. S. Taylor, A. D. Turnbull, A. M. Garofalo, M. A. Makowski,

- B. W. Rice, M. S. Chance, L. R. Baylor, M. Murakami, and M. R. Wade, *Physics of Plasmas* **7** (2000).
- [20] L. Lao, Y. Kamada, T. Oikawa, L. R. Baylor, K. Burrell, V. Chan, M. Chance, M. Chu, J. Ferron, T. Fukuda, *et al.*, *Nuclear fusion* **41**, 295 (2001).
- [21] A. W. Leonard, T. A. Casper, R. J. Groebner, T. H. Osborne, P. B. Snyder, and D. M. Thomas (2007).
- [22] A. Nelson, C. Paz-Soldan, and S. Saarelma, *Nuclear Fusion* **62**, 096020 (2022).
- [23] K. Imada, T. H. Osborne, S. Saarelma, J. G. Clark, A. Kirk, M. Knolker, R. Scannell, P. B. Snyder, V. C., and H. R. Wilson, *Nuclear Fusion* (2024).
- [24] C. T. Holcomb, J. R. Ferron, T. C. Luce, T. W. Petrie, P. A. Politzer, C. Challis, J. C. Deboo, E. J. Doyle, C. M. Greenfield, R. J. Groebner, M. Groth, A. W. Hyatt, G. L. Jackson, C. Kessel, R. J. L. Haye, M. A. Makowski, G. R. McKee, M. Murakami, T. H. Osborne, J. M. Park, R. Prater, G. D. Porter, H. Reimerdes, T. L. Rhodes, M. W. Shafer, P. B. Snyder, A. D. Turnbull, and W. P. West (2009).
- [25] T. Mau, S. Jardin, C. Kessel, J. Menard, R. Miller, F. Najmabadi, V. Chan, L. Lao, T. Petrie, P. Politzer, and A. Turnbull, in *18th IEEE/NPSS Symposium on Fusion Engineering* (1999) pp. 45–48.
- [26] S. Jardin, C. Kessel, J. Menard, T. Mau, R. Miller, F. Najmabadi, V. Chan, L. Lao, Y. Linliu, R. Miller, T. Petrie, P. Politzer, and A. Turnbull, *Fusion Engineering and Design* **65**, 165 (2003).
- [27] L. Bromberg, S. Pourrahimi, J. H. Schultz, P. Titus, S. Jardin, C. Kessel, and W. Reiersen, *Fusion Engineering and Design* **65** (2003).
- [28] J. E. Menard, T. Brown, L. El-Guebaly, M. Boyer, J. Canik, B. Colling, R. Raman, Z. Wang, Y. Zhai, P. Buxton, B. Covele, C. D’Angelo, A. Davis, S. Gerhardt, M. Gryaznevich, M. Harb, T. C. Hender, S. Kaye, D. Kingham, M. Kotschenreuther, S. Mahajan, R. Maingi, E. Marriott, E. T. Meier, L. Mynsberge, C. Neumeyer, M. Ono, J. K. Park, S. A. Sabbagh, V. Soukhanovskii, P. Valanju, and R. Woolley, *Nuclear Fusion* **56**, 106023 (2016).
- [29] Y. K. Peng and D. J. Strickler, *Nuclear Fusion* **26** (1986).
- [30] D. Shafranov, *At. Energ.* **13** (1962).
- [31] H. Lütjens, A. Bondeson, and O. Sauter, *Computer Physics Communications* **97** (1996).
- [32] O. Sauter, C. Angioni, and Y. R. Lin-Liu, *Physics of Plasmas* **6** (1999).
- [33] A. Redl, C. Angioni, E. Belli, and O. Sauter, *Physics of Plasmas* **28** (2021), 10.1063/5.0012664.
- [34] J. Menard, S. Jardin, S. Kaye, C. Kessel, and J. Manickam, *Nuclear Fusion* **37**, 595 (1997).
- [35] T. H. Osborne, J. R. Ferron, R. J. Groebner, L. L. Lao, A. W. Leonard, M. A. Mahdavi, R. Maingi, R. L. Miller, A. D. Turnbull, M. Wade, and J. Watkins, *Plasma Physics and Controlled Fusion* **42** (2000).
- [36] P. B. Snyder, W. M. Solomon, K. H. Burrell, A. M. Garofalo, B. A. Grierson, R. J. Groebner, A. W. Leonard, R. Nazikian, T. H. Osborne, E. A. Belli, J. Candy, and H. R. Wilson, *Nuclear Fusion* **55** (2015).
- [37] J. F. Parisi, A. O. Nelson, R. Gaur, S. M. Kaye, F. I. Parra, J. W. Berkery, K. Barada, C. Clauser, A. J. Creely, A. Diallo, W. Guttenfelder, J. W. Hughes, L. A. Kogan, A. Kleiner, A. Q. Kuang, M. Lampert, T. Macwan, J. E. Menard, and M. A. Miller, “Kinetic-ballooning-bifurcation in tokamak pedestals across shaping and aspect-ratio (<https://arxiv.org/abs/2312.05216>),” (2023), arXiv:2312.05216 [physics.plasm-ph].
- [38] F. A. Haas, *Nuclear Fusion* **15** (1975).
- [39] E. A. Lazarus, J. B. Lister, and G. H. Neilson, *Nuclear Fusion* **30** (1990).
- [40] D. J. Ward, A. Bondeson, and F. Hofmann, *Nuclear Fusion* **33** (1993).
- [41] R. Sweeney, A. J. Creely, J. Doody, T. Fülöp, D. T. Garnier, R. Granetz, M. Greenwald, L. Hesslow, J. Irby, V. A. Izzo, R. J. L. Haye, N. C. Logan, K. Montes, C. Paz-Soldan, C. Rea, R. A. Tinguely, O. Vallhagen, and J. Zhu, *Journal of Plasma Physics* **86** (2020).
- [42] A. O. Nelson, D. T. Garnier, D. J. Battaglia, C. Paz-Soldan, I. Stewart, M. Reinke, A. J. Creely, and J. Wai, “Implications of vertical stability control on the sparc tokamak,” (2024), arXiv:2401.09613.
- [43] S. Guizzo, A. O. Nelson, C. Hansen, F. Logak, and C. Paz-Soldan, “Assessment of vertical stability for negative triangularity pilot plants,” (2024), arXiv:2401.15217 [physics.plasm-ph].
- [44] C. Hansen, I. Stewart, D. Burgess, M. Pharr, S. Guizzo, F. Logak, A. Nelson, and C. Paz-Soldan, *Computer Physics Communications* **298**, 109111 (2024).
- [45] D. Y. Lee, C. S. Chang, J. Manickam, N. Pomphrey, M. S. Chance, and S. C. Jardin, *Fusion Engineering and Design* **45** (1999).
- [46] D. A. Humphreys, T. A. Casper, N. Eidietis, M. Ferrara, D. A. Gates, I. H. Hutchinson, G. L. Jackson, E. Kolemen, J. A. Leuer, J. Lister, L. L. Lodestro, W. H. Meyer, L. D. Pearlstein, A. Portone, F. Sartori, M. L. Walker, A. S. Welander, and S. M. Wolfe, *Nuclear Fusion* **49** (2009).
- [47] P. F. Buxton, O. Asunta, M. P. Gryaznevich, D. Lockley, S. McNamara, S. Medvedev, E. R. D. V. Valdés, G. Whitfield, and J. M. Wood, *Plasma Physics and Controlled Fusion* **60** (2018).
- [48] F. Pesamosca, F. Felici, S. Coda, and C. Galperti, *Fusion Science and Technology* **78** (2022).
- [49] J. P. Lee, A. Cerfon, J. P. Freidberg, and M. Greenwald, *Journal of Plasma Physics* **81** (2015).
- [50] J. E. Menard, S. Gerhardt, M. Bell, J. Bialek, A. Brooks, J. Canik, J. Chrzanowski, M. Denault, L. Dudek, D. A. Gates, N. Gorelenkov, W. Guttenfelder, R. Hatcher, J. Hosea, R. Kaita, S. Kaye, C. Kessel, E. Kolemen, H. Kugel, R. Maingi, M. Mardenfeld, D. Mueller, B. Nelson, C. Neumeyer, M. Ono, E. Perry, R. Ramakrishnan, R. Raman, Y. Ren, S. Sabbagh, M. Smith, V. Soukhanovskii, T. Stevenson, R. Strykowski, D. Stutman, G. Taylor, P. Titus, K. Tresemer, K. Tritz, M. Viola, M. Williams, R. Woolley, H. Yuh, H. Zhang, Y. Zhai, and A. Zolfaghari, *Nuclear Fusion* **52** (2012).
- [51] M. E. Austin, A. Marinoni, M. L. Walker, M. W. Brookman, J. S. Degraessie, A. W. Hyatt, G. R. McKee, C. C. Petty, T. L. Rhodes, S. P. Smith, C. Sung, K. E. Thome, and A. D. Turnbull, *Physical Review Letters* **122**, 115001 (2019).
- [52] A. Nelson, L. Schmitz, C. Paz-Soldan, K. E. Thome, T. B. Cote, N. Leuthold, F. Scotti, M. E. Austin, A. Hyatt, and T. Osborne, *Physical Review Letters* **131**, 195101 (2023).
- [53] M. Shimada, D. J. Campbell, V. Mukhovatov, M. Fujiwara, N. Kirneva, K. Lackner, M. Nagami, V. D. Pustovitov, N. Uckan, J. Wesley, N. Asakura, A. E. Costley, A. J. Donné, E. J. Doyle, A. Fasoli, C. Gormezano,

- Y. Gribov, O. Gruber, T. C. Hender, W. Houlberg, S. Ide, Y. Kamada, A. Leonard, B. Lipschultz, A. Loarte, K. Miyamoto, V. Mukhovatov, T. H. Osborne, A. Polevoi, and A. C. Sips, *Nuclear Fusion* **47** (2007).
- [54] B. Sorbom, J. Ball, T. Palmer, F. Mangiarotti, J. Sierchio, P. Bonoli, C. Kasten, D. Sutherland, H. Barnard, C. Haakonsen, J. Goh, C. Sung, and D. Whyte, *Fusion Engineering and Design* **100**, 378 (2015).
- [55] D. G. Whyte, J. Minervini, B. LaBombard, E. Marmor, L. Bromberg, and M. Greenwald, *Journal of Fusion Energy* **35** (2016).
- [56] H. Zohm, *Philosophical Transactions of the Royal Society A: Mathematical, Physical and Engineering Sciences* **377** (2019).